

## Structure-Based Design, Synthesis, and in vitro Evaluation of Nonpeptidic Neprilysin Inhibitors

Stefan Sahli,<sup>[b]</sup> Bernhard Stump,<sup>[b]</sup> Tobias Welti,<sup>[b]</sup>  
Denise Blum-Kaelin,<sup>[a]</sup> Johannes D. Aebi,<sup>[a]</sup>  
Christian Oefner,<sup>[c]</sup> Hans-Joachim Böhm,<sup>\*[a]</sup> and  
François Diederich<sup>\*[b]</sup>

Neprilysin (NEP, neutral endopeptidase, EC 3.4.24.11) is a mammalian zinc(II)-dependent, membrane-bound endopeptidase. NEP is widely distributed in the organs, particularly in the kidneys and lungs, and is involved in the metabolism of a number of smaller regulatory peptides of the nervous, cardiovascular, inflammatory, and immune systems.<sup>[1–3]</sup> Enkephalins are among its natural substrates, and blocking NEP would increase their level, thereby generating an analgetic response. Furthermore, NEP cleaves ANP (atrial natriuretic peptide) and bradykinin, which both reduce blood pressure, and NEP inhibitors could therefore be possible antihypertensive agents. On the other hand, NEP has recently been shown to cleave amyloid  $\beta$ -peptide, the deposition of which in the brain is part of the initiation of Alzheimer's disease.<sup>[4]</sup> These therapeutic and basic pharmacological research interests led us to develop new nonpeptidic inhibitors of Neprilysin by X-ray structure-based de novo design.<sup>[5]</sup> Many peptidic NEP inhibitors are known,<sup>[2]</sup> but only a few nonpeptidic ones have been report-

[a] Dr. D. Blum-Kaelin, Dr. J. D. Aebi, Prof. Dr. H.-J. Böhm  
Pharma Research Basel, Discovery Chemistry, F. Hoffmann–La Roche Ltd.  
4070 Basel (Switzerland)  
Fax: (+41) 61-688-7408  
E-mail: hans-joachim.boehm@roche.com

ed.<sup>[6]</sup> Furthermore, we are interested in a general understanding of the structural requirements for selective metalloprotease inhibition, with the intriguing ultimate target of blocking NEP selectively and with high affinity without binding to the zinc(II) ion. Here, we report the synthesis and in vitro evaluation of first- and second-generation nonpeptidic Nephilysin inhibitors that still contain a zinc(II)-binding ligand and show  $IC_{50}$  values ( $IC_{50}$  = concentration of inhibitor at which 50%  $V_{max}$  is observed) in the range between 2 and 0.2  $\mu\text{M}$ .

On the basis of the X-ray crystal structure of NEP complexed with phosphoramidon,<sup>[7]</sup> we used the molecular-modeling package MOLOC<sup>[8]</sup> to analyze the active site and to design the well-accommodated lead ( $\pm$ )-1, taking into account the principles of molecular recognition. Figure 1 shows that the central imidazole platform of the active ( $1'S,1''R$ )-configured enantiomer should act as a peptide-bond isoster and anchor at the active site by forming H-bonds to Asn542 and Arg717, both of which are important for substrate binding.<sup>[9,10]</sup> Two aromatic rings, attached by short linkers to positions 2 and 5 of the central imidazole scaffold, were expected to fill the hydrophobic pockets  $S1'$  and  $S2'$ . A thiol ligand was chosen to ensure binding to the catalytically active zinc(II) ion. In addition to ( $\pm$ )-1, we also prepared compounds ( $\pm$ )-2–( $\pm$ )-5 in the first lead-generation cycle.

The synthesis of the first series of ligands elegantly takes advantage of a double *ortho*-metallation strategy (Scheme 1).<sup>[12]</sup> Protected imidazole **6**<sup>[13]</sup> was stannylated at position 2, and Stille cross-coupling with (*Z*)-2-bromo-3-phenylprop-3-enal afforded aldehyde **7**. Reduction of aldehyde and double bond with  $[Pd(PPh_3)_4]$  and  $Bu_3SnH$  in one step, followed by silylation provided the silyl ether ( $\pm$ )-**8**. Metallation at position 5 of the imidazole ring followed by treatment with benzaldehyde led to the diastereomeric pairs of enantiomers ( $\pm$ )-**9a** and ( $\pm$ )-**9b**. Methylation of the hydroxy group followed by desilylation yielded ( $\pm$ )-**10a** and ( $\pm$ )-**10b**. At this stage, the diastereoisomers were separated by column chromatography ( $SiO_2$ , pentane/ $AcOEt$  50:50). Mitsunobu reaction provided the thioacetates ( $\pm$ )-**11a** and ( $\pm$ )-**11b** that were finally doubly deprotected to afford thiols ( $\pm$ )-**1** and ( $\pm$ )-**2**.<sup>[14,15]</sup> The configuration of the separated diastereoisomers was assigned based on an X-ray crystal structure of thioacetate ( $1'SR,1''RS$ )-**11a**. The other inhibitors ( $\pm$ )-**3** to ( $\pm$ )-**5** were obtained by similar routes.

The  $IC_{50}$  values were determined by a fluorimetric assay.<sup>[16]</sup> Encouragingly, the activity of lead com-

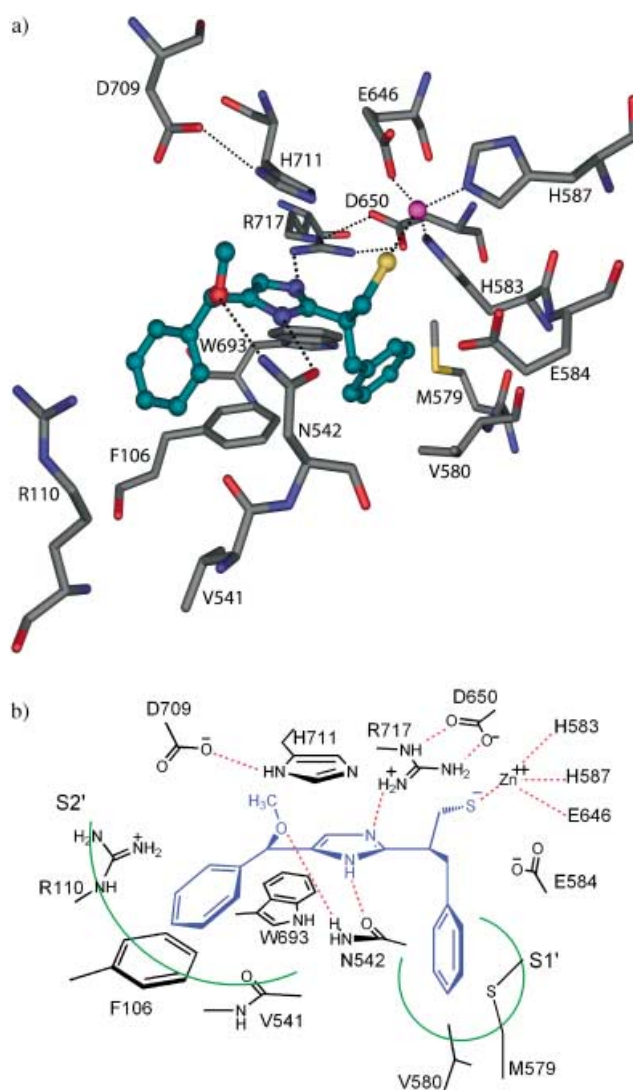
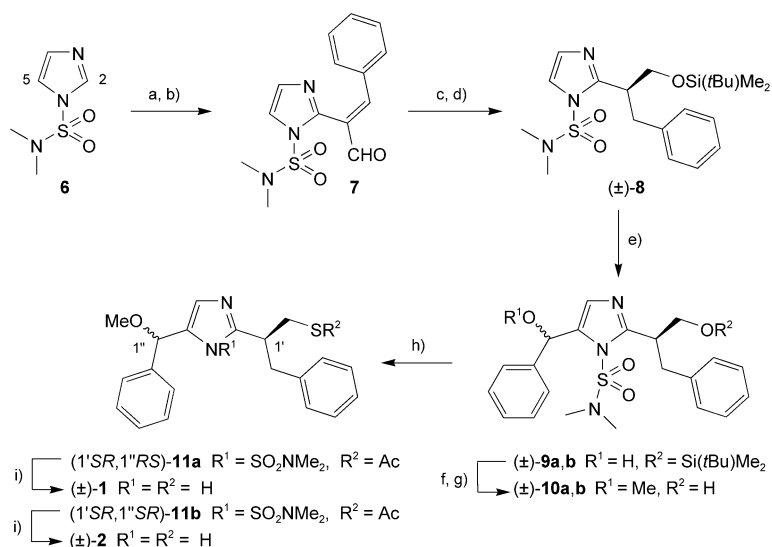


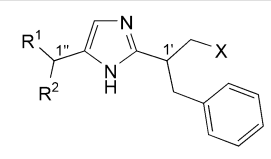
**Figure 1.** Ball-and-stick (a) and schematic (b) representations of ( $1'S,1''R$ )-**1** modeled in the active site of Nephilysin. Potential H-bonds are shown as dashed lines. a) C atoms of the inhibitor: green, C atoms of NEP: grey, O atoms: red, N atoms: blue, S atoms: yellow, Zn atom: purple.



**Scheme 1.** Synthesis of inhibitors ( $\pm$ )-**1** and ( $\pm$ )-**2**. Reagents and conditions: a)  $nBuLi$ ,  $Bu_3SnCl$ ,  $THF$ ,  $-78^\circ C$ ; b) (*Z*)-2-Bromo-3-phenylprop-3-enal,  $[Pd(PPh_3)_2Cl_2]$ ,  $Ag_2O$ ,  $DMF$ ,  $100^\circ C$ , 2 d, 40% (two steps); c)  $[Pd(PPh_3)_4]$ ,  $Bu_3SnH$ ,  $AcOH$ ,  $PhH$ ,  $20^\circ C$ , 10 h, 82%; d)  $Me_3(tBu)SiCl$ ,  $DMAP$ ,  $CH_2Cl_2$ ,  $20^\circ C$ , 16 h, 79%; e)  $secBuLi$ ,  $PhCHO$ ,  $THF$ ,  $-78^\circ C$ , 1 h, 85%; f)  $NaH$ ,  $MeI$ ,  $THF$ ,  $0 \rightarrow 20^\circ C$ , 98%; g)  $Bu_4NF$ ,  $THF$ ,  $20^\circ C$ , 4 h, 62% ( $(\pm)$ -**10a**), 35% ( $(\pm)$ -**10b**); h)  $PPh_3$ ,  $DIAD$ ,  $AcSH$ ,  $THF$ ,  $0 \rightarrow 20^\circ C$ , 3 h, 95% ( $(1'SR,1''RS)$ -**11a**), 86% ( $(1'SR,1''SR)$ -**11b**); i)  $NaOMe$ ,  $MeOH$ ,  $20^\circ C$ , 1 h then  $TFA$ ,  $20^\circ C$ , 1 h, then 0.1%  $HCl$  in  $MeOH$ , 30% ( $(\pm)$ -**1**), 28% ( $(\pm)$ -**2**).  $DMAP$  = 4-(dimethylamino)pyridine,  $DIAD$  = diisopropyl azodicarboxylate,  $TFA$  = trifluoroacetic acid.

compound ( $\pm$ )-1 was found to be in the single-digit micromolar range (Table 1). Similar  $IC_{50}$  values around  $2 \mu\text{M}$  obtained for inhibitors ( $\pm$ )-1 and ( $\pm$ )-2 demonstrate that the proposed H-bond between Asn542 and the methoxy group in the complex of ( $\pm$ )-1 is not effective; indeed the H-bond-accepting residue can be omitted without penalty as in ( $\pm$ )-3. Substitution of the phenyl (in ( $\pm$ )-1) by a 2-naphthyl ring (in ( $\pm$ )-4) for occupation of the  $S2'$  pocket does not enhance binding affinity but rather leads to a slightly lower activity. Although spacious and rather hydrophobic, this pocket is conformationally not as well defined (see below),<sup>[7,17]</sup> this prevents a gain in binding free enthalpy upon introduction of a larger substituent such as a

**Table 1.** Structures and biological activities of the first series of lead compounds ( $\pm$ )-1 to ( $\pm$ )-5. The configuration of the active enantiomer, predicted by modeling, is indicated.

					
	X	R <sup>1</sup>	R <sup>2</sup>	active enantiomer	$IC_{50}$ [ $\mu\text{M}$ ]
( $\pm$ )-1	SH	OMe	Ph	1'S,1''R	2.0
( $\pm$ )-2	SH	OMe	Ph	1'S,1''S	1.7
( $\pm$ )-3	SH	H	Ph	1'S	2.5
( $\pm$ )-4	SH	OMe	Np <sup>[a]</sup>	1'S,1''R	3.6
( $\pm$ )-5	OH	OMe	Ph	1'S,1''R	– <sup>[b]</sup>

[a] Np = 2-naphthyl. [b] 17% inhibition at 100  $\mu\text{M}$  inhibitor concentration.

naphthyl residue. Finally, alcohol ( $\pm$ )-5 proved to be almost inactive; this clearly shows that at this stage, a thiolate group is required for binding.

For the next lead-optimization cycle, we carefully compared the active site geometries seen in the X-ray crystal structures of NEP bound to the larger phosphoramidon (blue in Figure 2a), that occupies both  $S1'$  and  $S2'$  pockets, and the smaller thiorphan (green in Figure 2a), that only fills the  $S1'$  pocket.<sup>[18,19]</sup> In the thiorphan complex, the  $S2'$  pocket is closed by the side chains of Arg110 and Phe106. Since good inhibitory activity apparently does not require occupancy of the  $S2'$  pocket,<sup>[6]</sup> second-generation ligands (+)-12 and (+)-13 were designed without a vector reaching into this pocket (Table 2). In return, larger heterocycles, benzimidazole in (+)-12 and imidazo[4,5-c]pyridine in (+)-13, were introduced as central scaffolds. Molecular modeling suggested that these platforms would not only undergo the obligatory H-bonding to Arg717 and Asn542, but would also engage in favorable  $\pi$ - $\pi$  stacking interactions<sup>[20]</sup> with the imidazole ring of His711 (Figure 2b).

The synthesis of thiols (+)-(S)-12 and (+)-(S)-13 started from carboxylic acid (–)-(S)-16 that was obtained through a published protocol (Scheme 2).<sup>[21]</sup> Formation of the carboxamide with either 1,2-phenylenediamine or 3,4-diaminopyridine, followed by acid-catalyzed condensation to give (+)-15/(+)-17 and *S*-deprotection afforded the desired ligands.

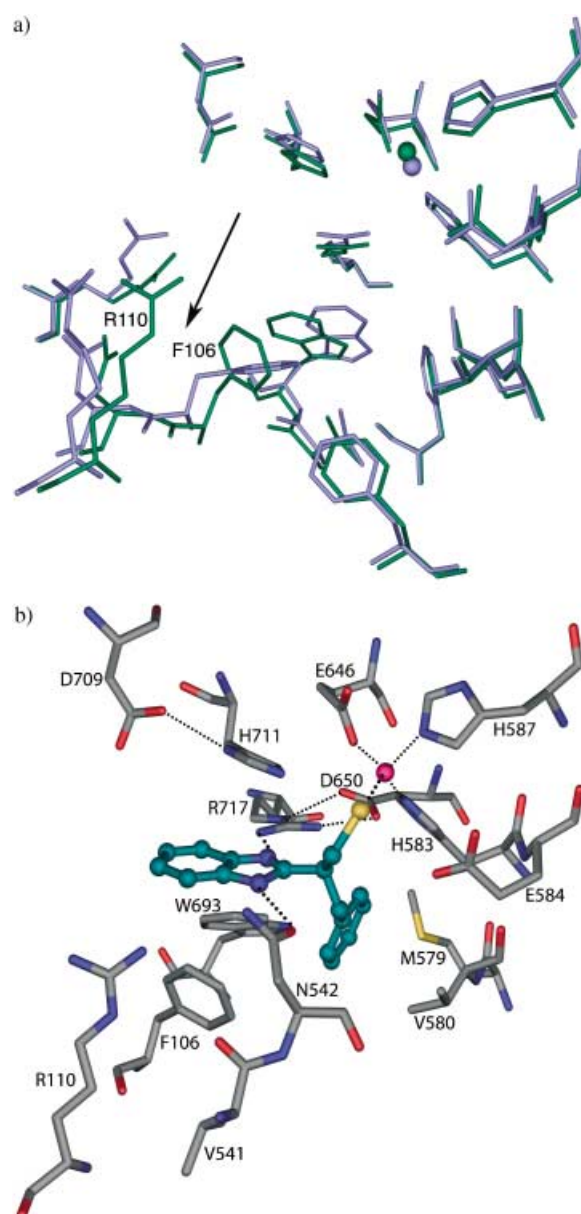


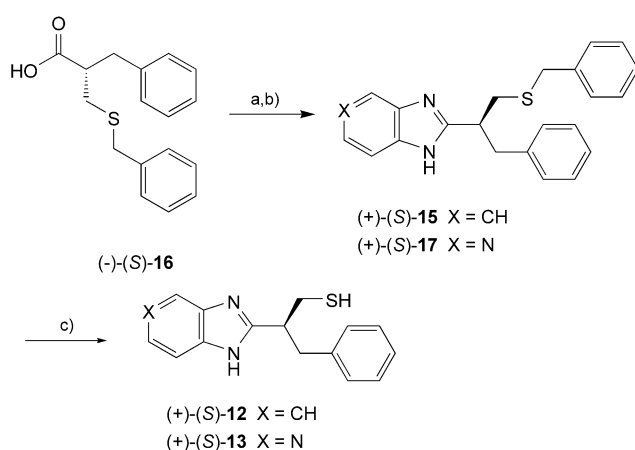
**Figure 2.** a) Superimposed active site residues seen in the X-ray crystal structures of NEP complexed with phosphoramidon (blue) and thiorphan (green). The inhibitors are not shown for clarity. In the thiorphan complex, the  $S2'$  pocket remains closed as indicated by the arrow. b) Ball-and-stick representation of the predicted binding of (+)-12 in the active site of Neprilysin. Potential H-bonds are shown as dashed lines.

Gratifyingly, the  $IC_{50}$  values of the new ligands (+)-12 and (+)-13 were in the upper nanomolar range, their binding affinity being about tenfold higher than that of the imidazole-based inhibitors (Table 2). Benzimidazole and imidazo[4,5-c]pyridine appear to be excellent new scaffolds for NEP inhibitors. Their predicted aromatic interaction with the imidazole ring of His711 still remains to be validated by X-ray crystallography. For comparison, the binding affinity of benzylated (+)-15 is poor, although, according to the modeling, the benzyl residue can be well accommodated in the active site. Thus, a thiolate ligand to the zinc(II) ion is still required at this stage. The affini-

**Table 2.** Structures and biological activities of the second-generation lead compounds (+)-12 and (+)-13 and the corresponding controls (+)-14 and (+)-15.

	X	R <sup>1</sup>	R <sup>2</sup>	IC <sub>50</sub> [μM]
(+)-(S)-12	CH	H	H	0.29
(+)-(S)-13	N	H	H	0.20
(+)-(S)-14	CH	Me	H	5.3
(+)-(S)-15	CH	H	Bn <sup>[a]</sup>	— <sup>[b]</sup>

[a] Bn = benzyl. [b] 30% inhibition at 100 μM inhibitor concentration.



**Scheme 2.** Synthesis of inhibitors (+)-12 and (+)-13. Reagents and conditions: a) 4-Methylmorpholine, *i*BuOCOCl, 1,2-phenylenediamine or 3,4-diaminopyridine, THF,  $-20 \rightarrow 0^\circ\text{C}$ , 14 h, 47–51%; b) AcOH,  $65^\circ\text{C}$ , 4 h, 90% ((+)-15), 92% ((+)-17); c) Na, NH<sub>3</sub>, THF,  $-78^\circ\text{C}$ , 10 min, 50% ((+)-12), 40% ((+)-13).

ty of the *N*-methylated benzimidazole (+)-14 was 20-fold reduced relative to (+)-12. This result provides strong support for the prediction that the imidazole moiety in the heterocyclic scaffolds of (+)-12 and (+)-13 acts as peptide-bond isoster and undergoes H-bonding to the side chains of both Asn542 and Arg717. Apparently, for steric reasons, the *N*-methyl derivative does not fit ideally into the narrow site between Asn542 and Arg717 and hence is not well positioned for forming a good H-bond to Arg717.

In conclusion, benzimidazole and imidazo[4,5-*c*]pyridine represent excellent new scaffolds for NEP inhibitors that are available by short, versatile synthetic routes. Their imidazole moiety seems to be a good peptide-bond isoster, undergoing H-bonding to both Asn542 and Arg717. We hope to further validate the proposed binding mode, which is well supported by the experimental data, by X-ray analysis. The comparison between the first imidazole series of ligands (i.e. (±)-1–(±)-3) and the second-generation inhibitors underlines the fact that occupation of the S2' pocket is energetically not beneficial, in contrast to filling the S1' pocket. Further optimization of the S1' residue should lead to highly potent inhibitors,<sup>[6]</sup> but modeling also suggests that the new extended heterocyclic scaffolds offer in-

teresting opportunities for exploring new bonding interactions "above" the S2' pocket. A thiolate ligand to the zinc(II) ion is still required at this stage; we hope, however, to develop in future work potent and selective inhibitors in which direct ligation to the zinc(II) ion will be substituted by H-bonding to the metal ion-bound catalytic water.

## Acknowledgements

We thank the ETH Research Council and F. Hoffmann–La Roche, Basel, for supporting this work.

**Keywords:** endopeptidases · inhibitors · medicinal chemistry · neprilysin · structure-based design

- [1] A. J. Turner, K. Tanzawa, *FASEB J.* **1997**, *11*, 355–364.
- [2] B. F. Roques, F. Noble, V. Daugé, M.-C. Fournié-Zaluski, A. Beaumont, *Pharmacol. Rev.* **1993**, *45*, 87–146.
- [3] A. J. Turner, R. E. Isaac, D. Coates, *BioEssays* **2001**, *23*, 261–269.
- [4] N. Iwata, S. Tsubuki, Y. Takaki, K. Shirotani, B. Lu, N. P. Gerard, C. Gerard, E. Hama, H. J. Lee, T. C. Saïdo, *Science* **2001**, *292*, 1550–1552.
- [5] For previous examples of X-ray structure-based de novo design of non-peptidic enzyme inhibitors, see: a) U. Obst, V. Gramlich, F. Diederich, L. Weber, D. W. Banner, *Angew. Chem.* **1995**, *107*, 1874–1877; *Angew. Chem. Int. Ed. Engl.* **1995**, *34*, 1739–1742; b) B. Masjost, P. Ballmer, E. Borroni, G. Zürcher, F. K. Winkler, R. Jakob-Roetne, F. Diederich, *Chem. Eur. J.* **2000**, *6*, 971–982; c) E. A. Meyer, R. Brenk, R. K. Castellano, M. Furler, G. Klebe, F. Diederich, *ChemBioChem* **2002**, *3*, 250–253; d) D. A. Carcache, S. R. Hörtner, A. Bertogg, C. Binkert, D. Bur, H. P. Märki, A. Dorn, F. Diederich, *ChemBioChem* **2002**, *3*, 1137–1141.
- [6] S. De Lombaert, L. Blanchard, J. Tan, Y. Sakane, C. Berry, R. D. Ghai, *Bioorg. Med. Chem. Lett.* **1995**, *5*, 145–150.
- [7] C. Oefner, A. D'Arcy, M. Henning, F. K. Winkler, G. E. Dale, *J. Mol. Biol.* **2000**, *296*, 341–349.
- [8] a) P. R. Gerber, K. Müller, *J. Comput.-Aided Mol. Des.* **1995**, *9*, 251–268; b) Gerber Molecular Design (<http://www.moloc.ch>).
- [9] N. Dion, H. Le Moual, M.-C. Fournié-Zaluski, B. P. Roques, P. Crine, G. Boileau, *Biochem. J.* **1995**, *311*, 623–627.
- [10] C. Marie-Claire, E. Ruffet, S. Antonczak, A. Beaumont, M. O'Donohue, B. P. Roques, M.-C. Fournié-Zaluski, *Biochemistry* **1997**, *36*, 13938–13945.
- [11] A. J. Gutierrez, T. J. Terhorst, M. D. Matteucci, B. C. Froehler, *J. Am. Chem. Soc.* **1994**, *116*, 5540–5544.
- [12] All new compounds were fully characterized by <sup>1</sup>H and <sup>13</sup>C NMR spectroscopy, FTIR spectroscopy, EI- or MALDI-MS, and elemental analysis or high-resolution MS. For optically active ligands and precursors, optical rotations were also measured, and the enantiomeric purity checked by HPLC on chiral stationary phase. The X-ray crystal structure analysis of (1'S,1''RS)-11a will be published as part of a forthcoming full paper.
- [13] D. J. Chadwick, R. I. Ngochindo, *J. Chem. Soc. Perkin Trans. 1* **1984**, 481–486.
- [14] O. Mitsunobu, *Synthesis* **1981**, 1–28.
- [15] L. Zervas, I. Photaki, N. Ghelis, *J. Am. Chem. Soc.* **1963**, *85*, 1337–1341.
- [16] K. M. Carvalho, G. Boileau, A. C. M. Camargo, L. Juliano, *Anal. Biochem.* **1996**, *237*, 167–173. The NEP assay was based on the method described by Carvalho et al. with a minor difference in the substrate. The fluorescent substrate (ABZ-GG<sub>5</sub>FLRRVQEDDnp) contained an additional glutamate between the valine and the fluorescent group. Incubations (for 1 h at 37°C) were carried out in 96-well microplates in triplicate at 4 to 6 concentrations ranging from 100 μM to 1 nM. IC<sub>50</sub> values were calculated after logit/log transformation of the percent inhibition data with a best-fit regression model. The inhibitors were tested for their fluorescence or quenching properties and values were corrected accordingly. Thiophan as reference compound gave an IC<sub>50</sub> of 7.0 ± 0.2 nM (*n* = 6) in this assay.

- [17] R. Bohacek, S. De Lombaert, C. McMartin, J. Priestle, M. Grütter, *J. Am. Chem. Soc.* **1996**, *118*, 8231–8249.
- [18] B. P. Roques, M.-C. Fournié-Zaluski, E. Soroça, J. M. Lecomte, B. Malfroy, C. Llorens, J. C. Schwartz, *Nature* **1980**, *288*, 286–288.
- [19] C. Oefner, F. Hoffmann–La Roche, Basel, unpublished results.
- [20] E. A. Meyer, R. K. Castellano, F. Diederich, *Angew. Chem.* **2003**, *115*, 1244–1287; *Angew. Chem. Int. Ed.* **2003**, *42*, 1210–1250.
- [21] D. A. Evans, D. J. Mathre, W. L. Scott, *J. Org. Chem.* **1985**, *50*, 1830–1835.
- 

Received: January 12, 2004